Analysis of Self-Emission from Spherical Shock Experiments

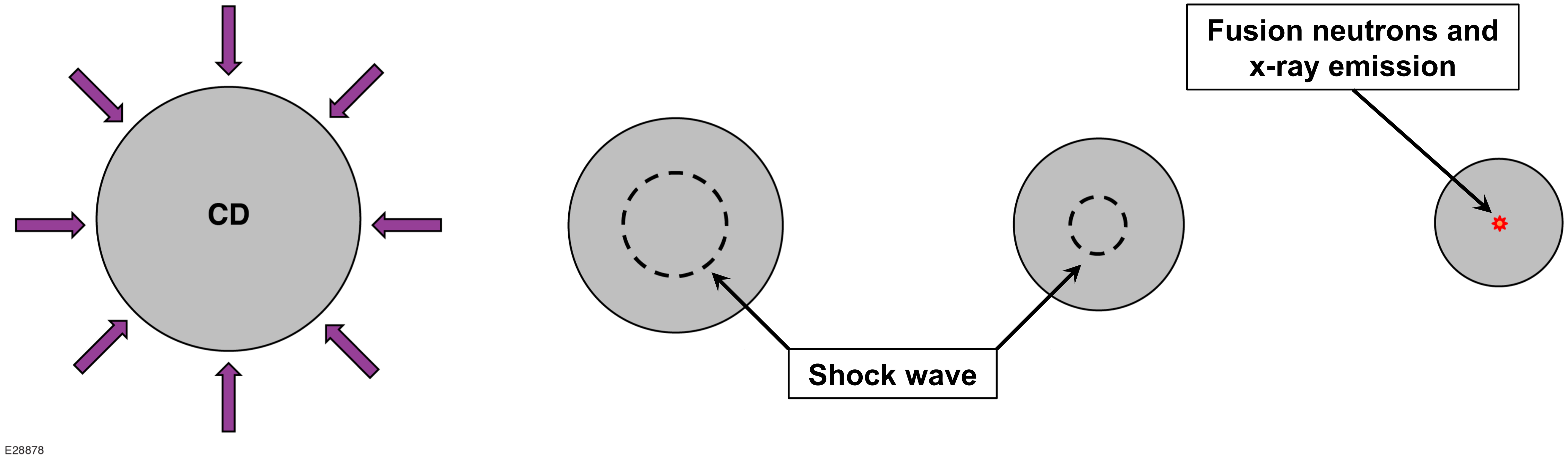

J. J. Ruby
University of Rochester
Laboratory for Laser Energetics

61st Annual Meeting of the
American Physical Society
Division of Plasma Physics
Fort Lauderdale, FL
21–25 October 2019

Experimental observations from spherical shock experiments are used to benchmark physics models in the multi-gigabar regime

UR LLE

- A spherical shock wave is driven in a solid deuterated plastic ball and the neutron and x-ray self emission are measured from the shock collapse
- A statistical method that includes physical and experimental parameters is used to constrain physics models with experimental data
- Preliminary analysis shows that models cannot reproduce experimental data without adjustment to physical parameters (laser coupling, opacity, equation of state)

This methodology provides a path to benchmark physics models in the multi-gigabar regime.

Collaborators

J. R. Rygg, D. A. Chin, C. J. Forrest, V. Yu. Glebov, C. Stoeckl, and G. W. Collins

University of Rochester
Laboratory for Laser Energetics

B. Bachmann, J. A. Gaffney, and Y. Ping

Lawrence Livermore National Laboratory

N. V. Kabadi and P. Adrian

Plasma Science and Fusion Center
Massachusetts Institute of Technology

Statistical methods are being developed that allow a systematic comparison of integrated physics models to experimental data

- **Recently much work has been done in trying to improve the predictability[*] and extrapolation of implosion models by finding a mapping[**] between simulations and experiments**
- **While this provides greater predictive capability for experimental design,[†] it does not offer insight into deficiencies in the physics present in models**

This work aims to identify where there are deficiencies in the physics models.

*J. A. Gaffney *et al*., Phys. Plasmas 26, 082704 (2019).
** V. Gopalaswamy *et al*., Nature 565, 581 (2019).
† K. D. Humbird *et al*., Computer Science Archive, available at https://arxiv.org/abs/1812.06055 (2018).

The experimental setup includes a solid CD sphere with a CH outer layer

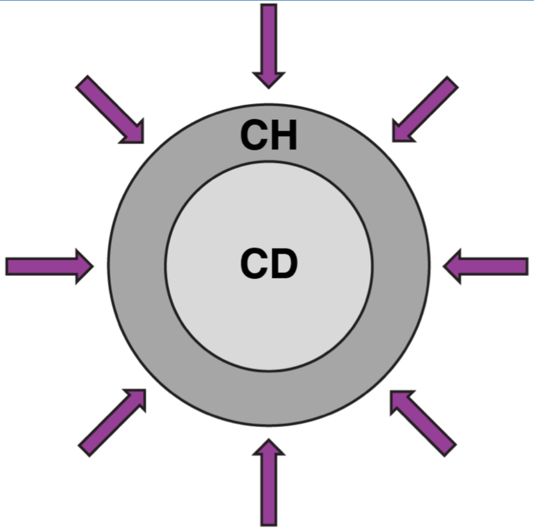

E28879

Parameter	Value
CD radius	436.9±2 μm
CH thickness	23.1±2 μm
CD composition	99.1±0.4 at. %
Laser energy	21.19±0.64 kJ
FC gate	40 ps±5 ps
FC pinholes	10 μm±0.5 μm
Pincam filters	15, 30, 50,100 μm Al ±10%
Pincam standoff	29.21±1.5 mm

Example experimental parameters

FC: framing camera
Pin: pinhole
SSD: smoothing by spectral dispersion

The OMEGA laser is used to drive a single spherically symmetric shock wave in a solid plastic ball at an initial pressure of about 40 Mbar

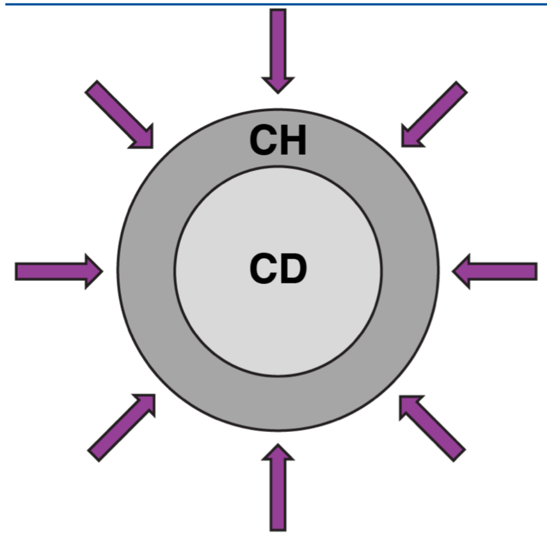

E28879

Parameter	Value
CD radius	436.9±2 μm
CH thickness	23.1±2 μm
CD composition	99.1±0.4 at. %
Laser energy	21.19±0.64 kJ
FC gate	40 ps±5 ps
FC pinholes	10 μm±0.5 μm
Pincam filters	15, 30, 50,100 μm Al ±10%
Pincam standoff	29.21±1.5 mm

Example experimental parameters

Average SSD pulse shape

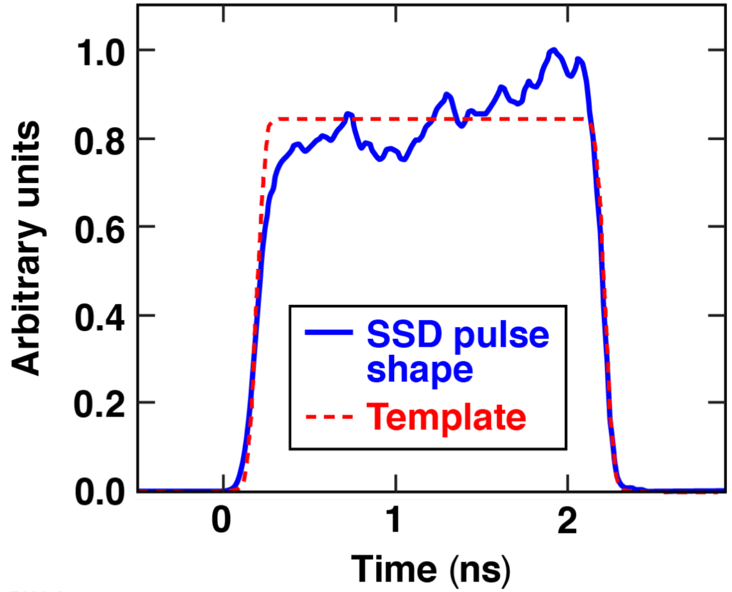

E28813

The OMEGA laser is used to drive a single spherically symmetric shock wave in a solid plastic ball at an initial pressure of about 40 Mbar

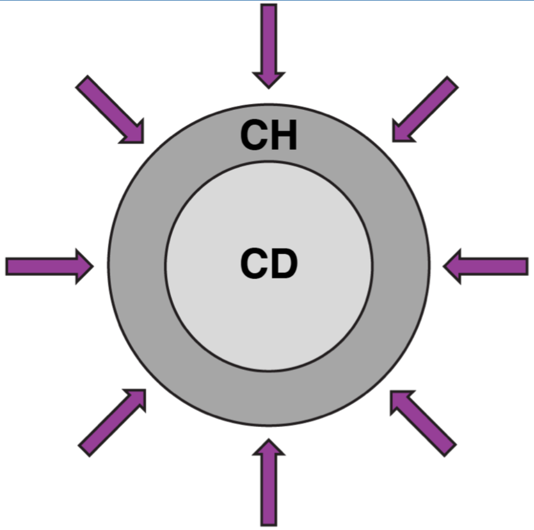

E28879

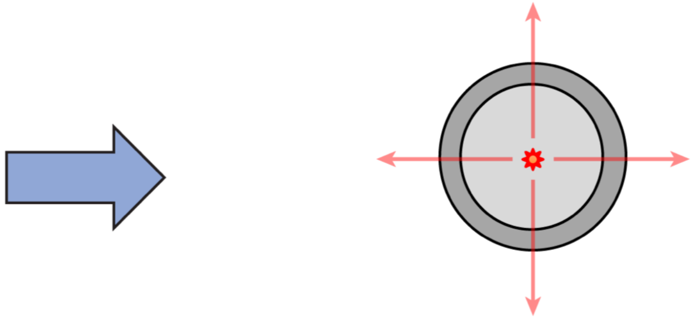

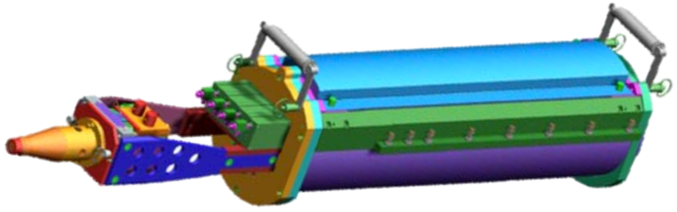

Parameter	Value
CD radius	436.9±2 μm
CH thickness	23.1±2 μm
CD composition	99.1±0.4 at. %
Laser energy	21.19±0.64 kJ
FC gate	40 ps±5 ps
FC pinholes	10 μm±0.5 μm
Pincam filters	15, 30, 50,100 μm Al ±10%
Pincam standoff	29.21±1.5 mm

Example experimental parameters

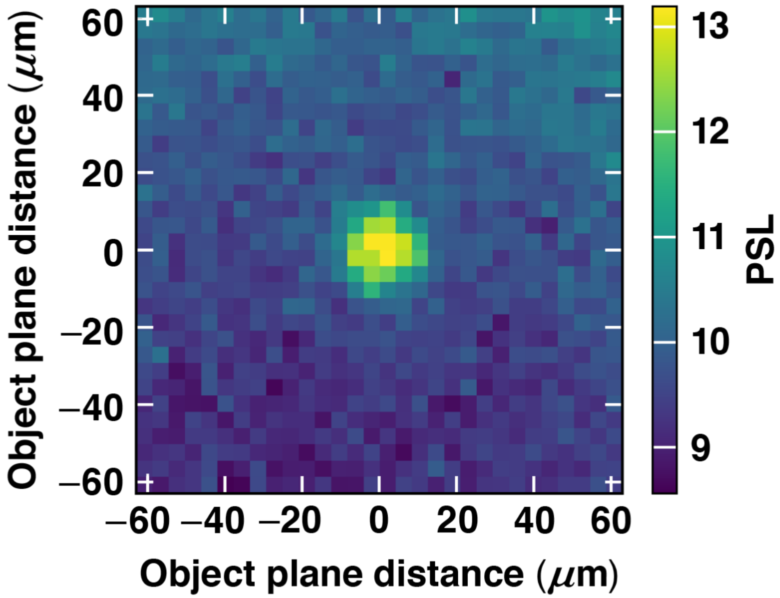

E28816

80 distinct experimental observables are measured

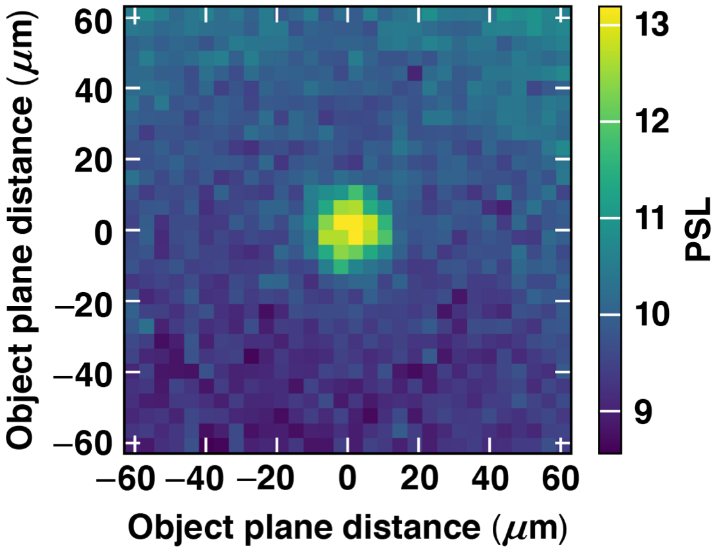

E28816

Spectrally spatially temporally resolved x-rays

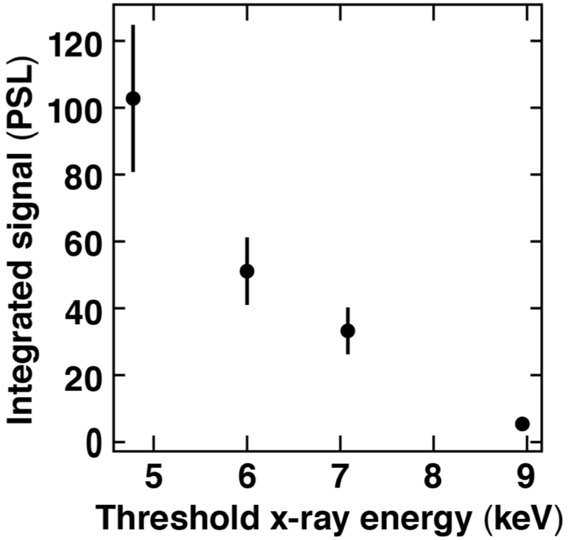

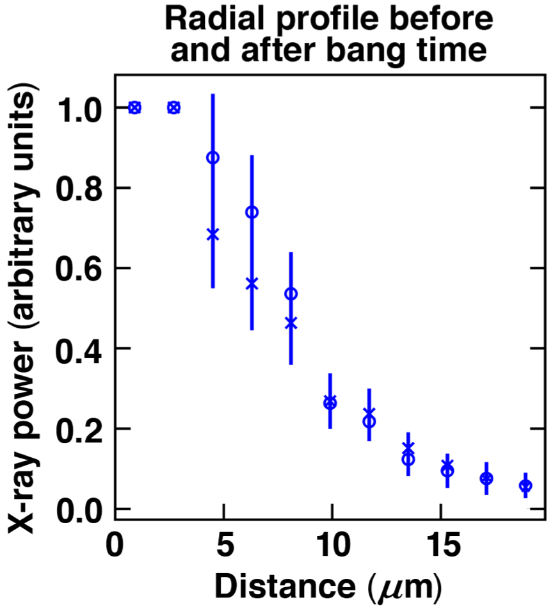

E28817

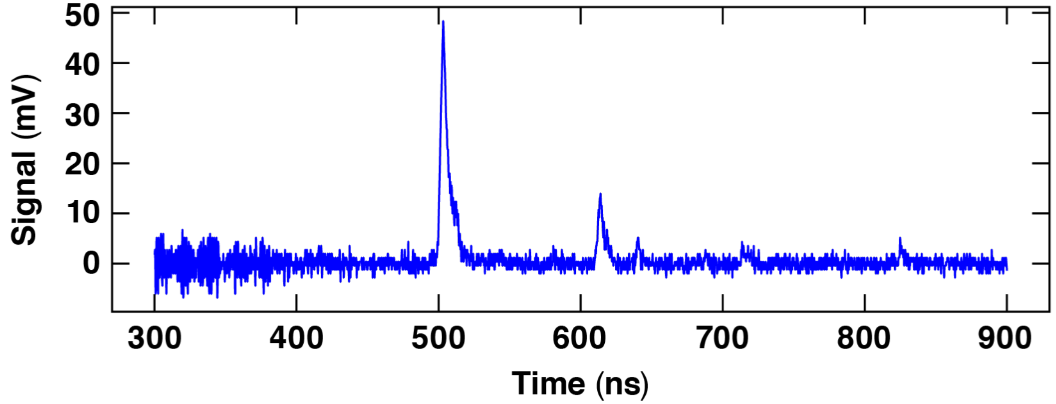

E28815

Neutron yield

	Value	Error
DD yield	2.59×10^5	1.61×10^5

The 80 experimental observations are compared to data modeled by the hydrodynamics code *LILAC* *

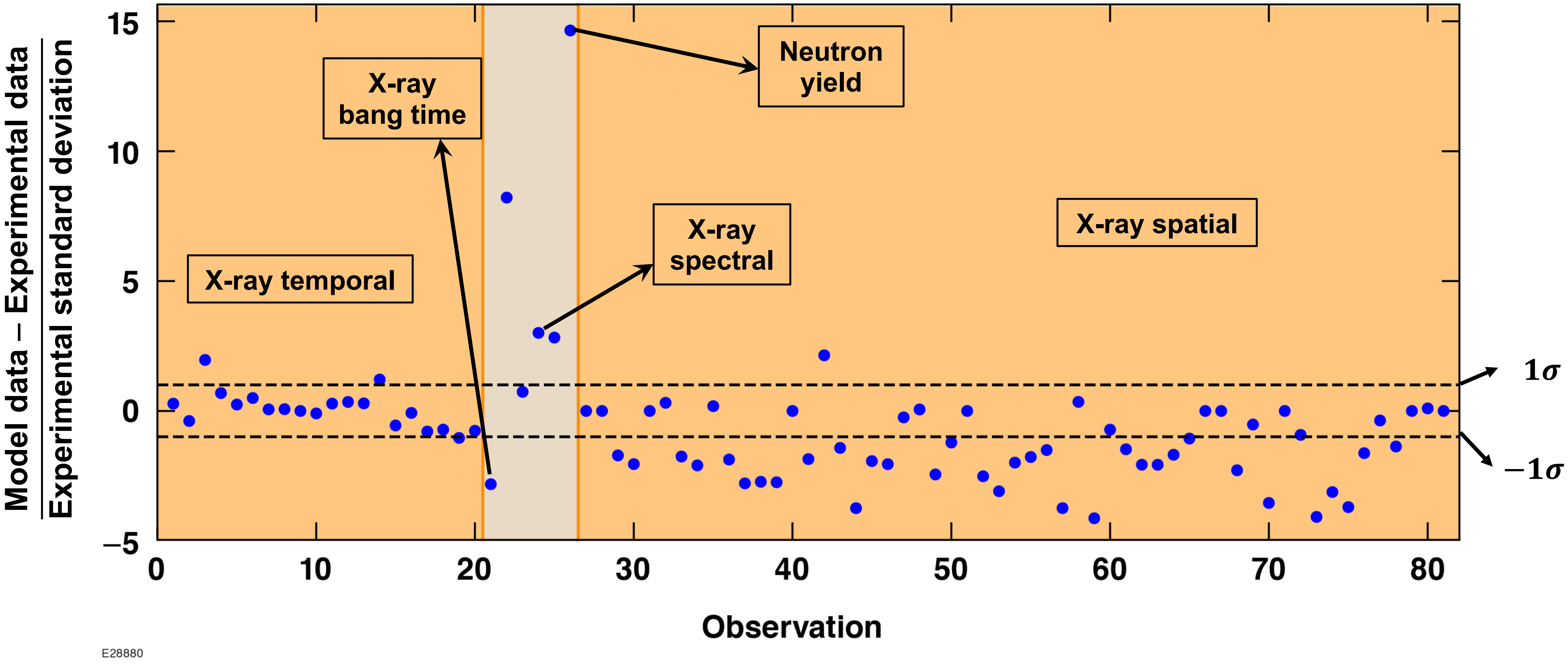

* J. Delettrez *et al.*, Phys. Rev. A 36, 3926 (1987).

A method developed by Gaffney *et al.*[*] that uses the information[**] as the objective function is used to fit the modeled data to the experimental data

- Gaffney *et al.*[*] developed a technique to constrain the physics of models by minimizing the information,[**] which is calculated from model predictions of experimental observations accounting for the effect of nuisance parameters from the experimental setup
- The information[**] consists of terms relating to:
  - standard χ^2 term
  - how much the difference in modeled data from observable data can be explained by variation in the nuisance parameters
  - information about nuisance parameters and prior information about physics parameters

* J. A. Gaffney *et al.*, Nucl. Fusion 53, 073032 (2013).
** C. E. Shannon, Bell Syst. Tech. J. 27, 623 (1948).

Physics parameters are adjusted until a minimum in the information is found

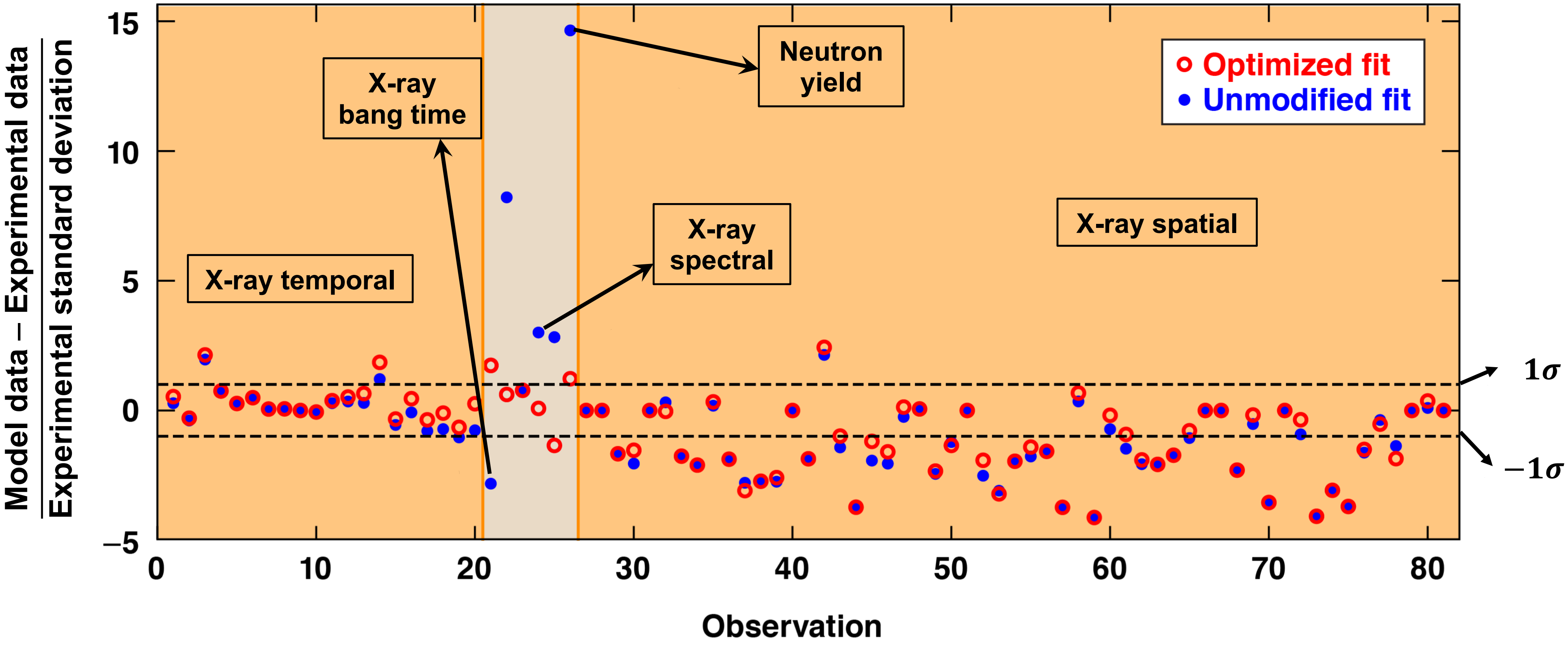

E28881

* J. Delettrez *et al.*, Phys. Rev. A 36, 3926 (1987).

The best fit includes an opacity multiplier of <1, indicating the opacity is overpredicted for x-ray energies above ~2 keV

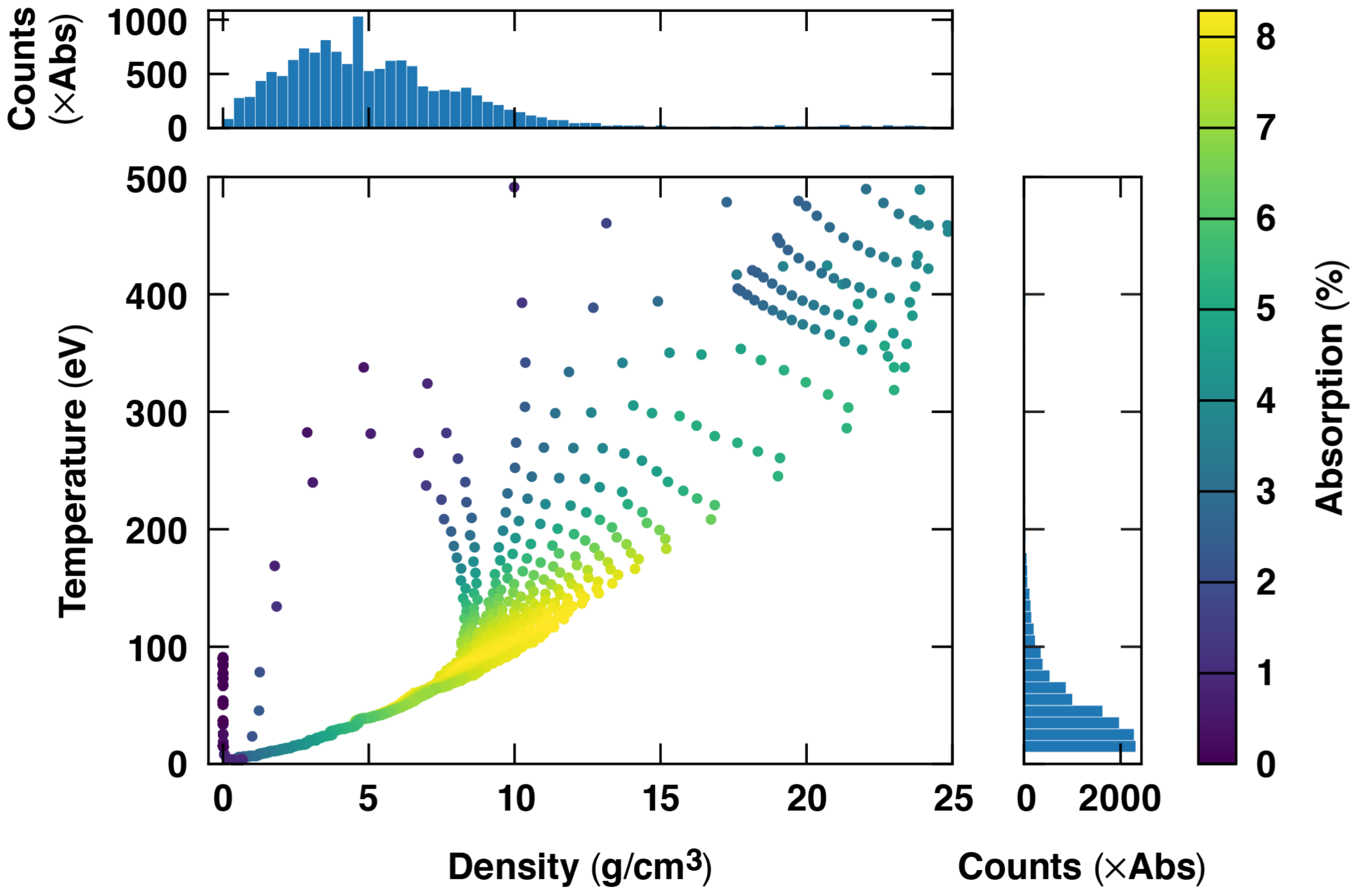

$$\boxed{f < 1}$$

$$= 100\% \left(e^{f\kappa\rho\Delta r} - 1\right)$$

The most absorption of hard x rays occurs in material that is around 5 g/cm^3 and 10 to 50 eV.

E28882

Experimental observations from spherical shock experiments are used to benchmark physics models in the multi-gigabar regime

- A spherical shock wave is driven in a solid deuterated plastic ball and the neutron and x-ray self emission are measured from the shock collapse
- A statistical method that includes physical and experimental parameters is used to constrain physics models with experimental data
- Preliminary analysis shows that models cannot reproduce experimental data without adjustment to physical parameters (laser coupling, opacity, equation of state)

This methodology provides a path to benchmark physics models in the multi-gigabar regime.

Backup slides

The physics parameters are varied and the shape of the information surface is mapped out searching for a minimum

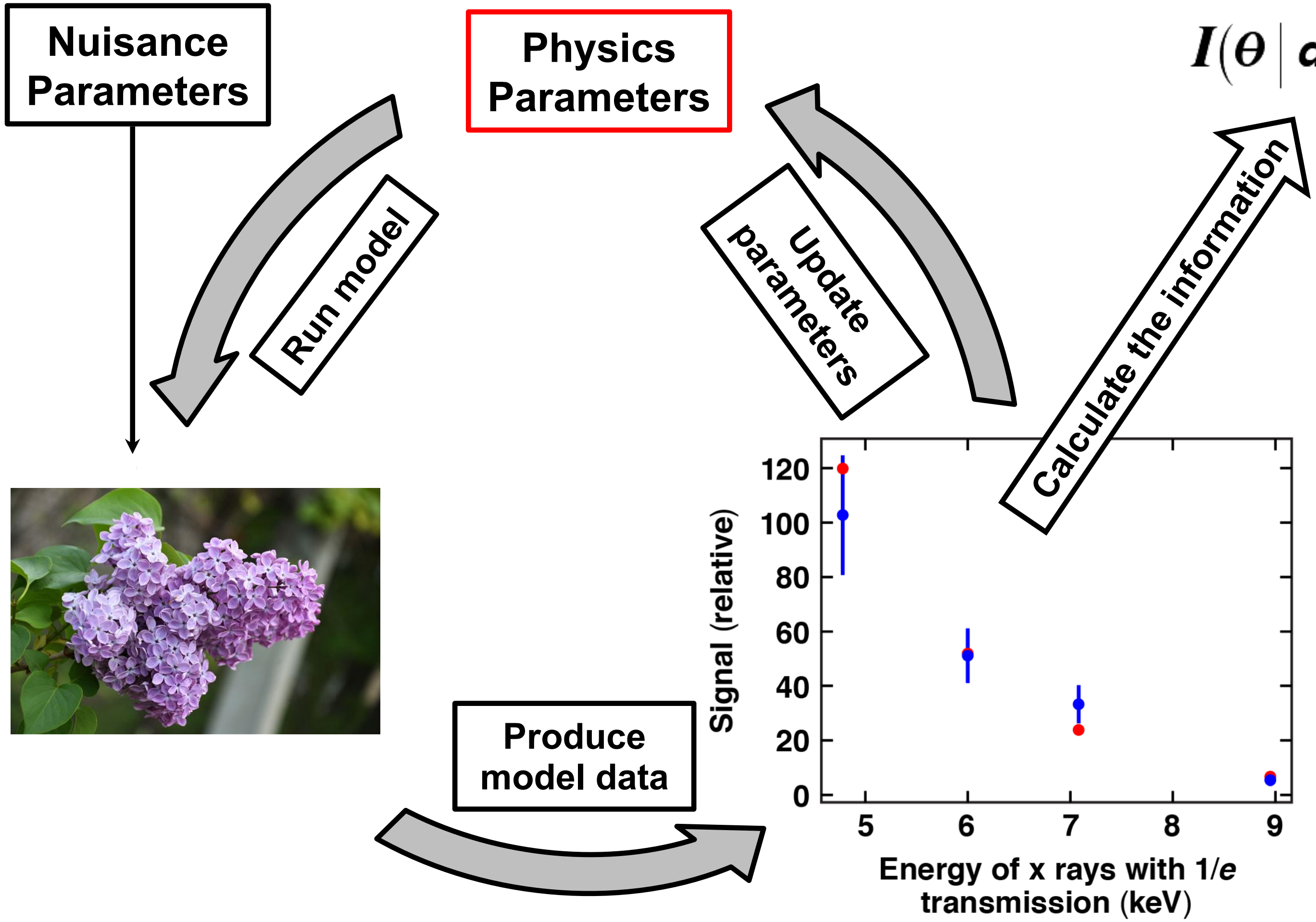

E28883

$$I(\theta \mid d_{\text{exp}})^{*} = \sum_i \frac{\left[d_{\text{exp},i} - d_{\text{m}}(\theta)_i\right]^2}{2\sigma^2_{\text{exp},i}} - \frac{1}{2}\left[d_{\text{exp}} - d_{\text{m}}(\theta)\right]^T \beta^T \beta \left[d_{\text{exp}} - d_{\text{m}}(\theta)\right] + \frac{1}{2}\ln\left(\left|\Lambda_\eta\right|\left|\alpha^T\alpha\right|\right) - \ln\left[P(\theta)\right]$$

- Standard χ^2 term
- How much the difference in modeled data from observable data can be explained by variation in the nuisance parameters
- Information about nuisance parameters and prior information about physics parameters

* J. A. Gaffney Nucl. Fusion. 53, 073032 (2013)

Coarse x-ray spectral measurements were made using a filtered x-ray pinhole camera

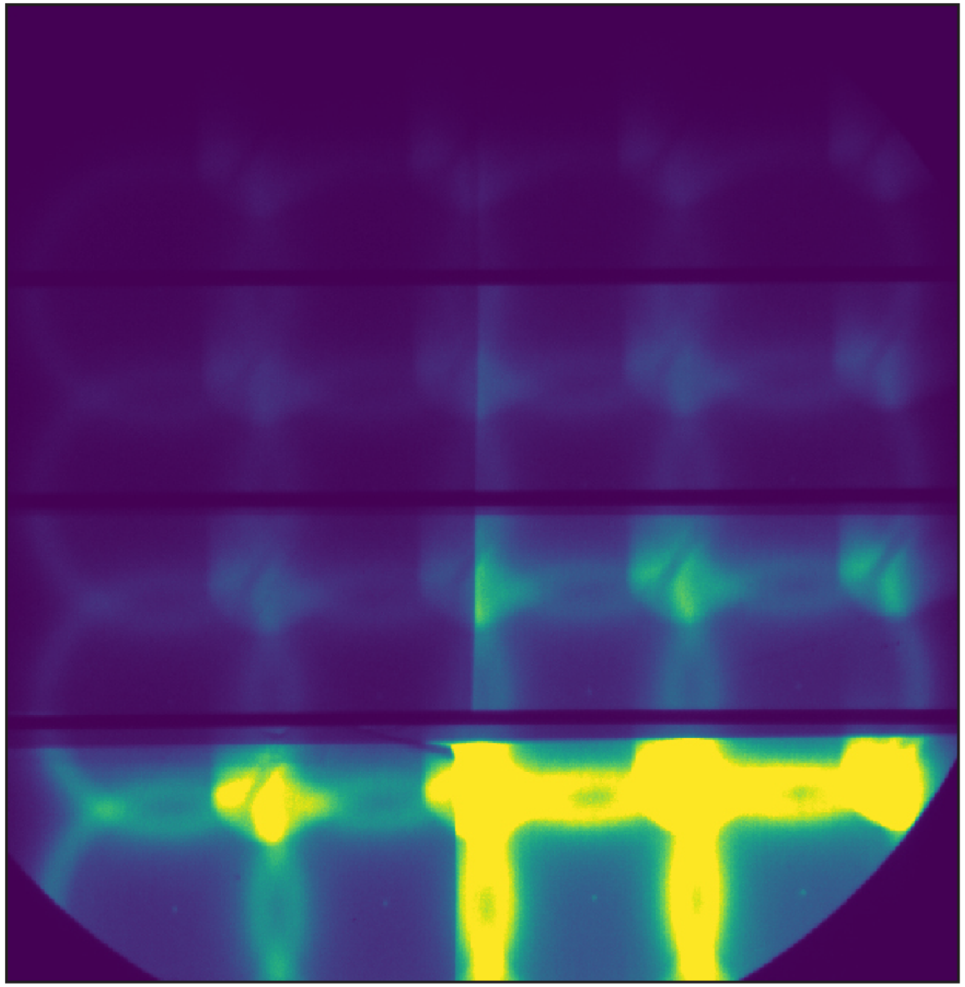

E28884

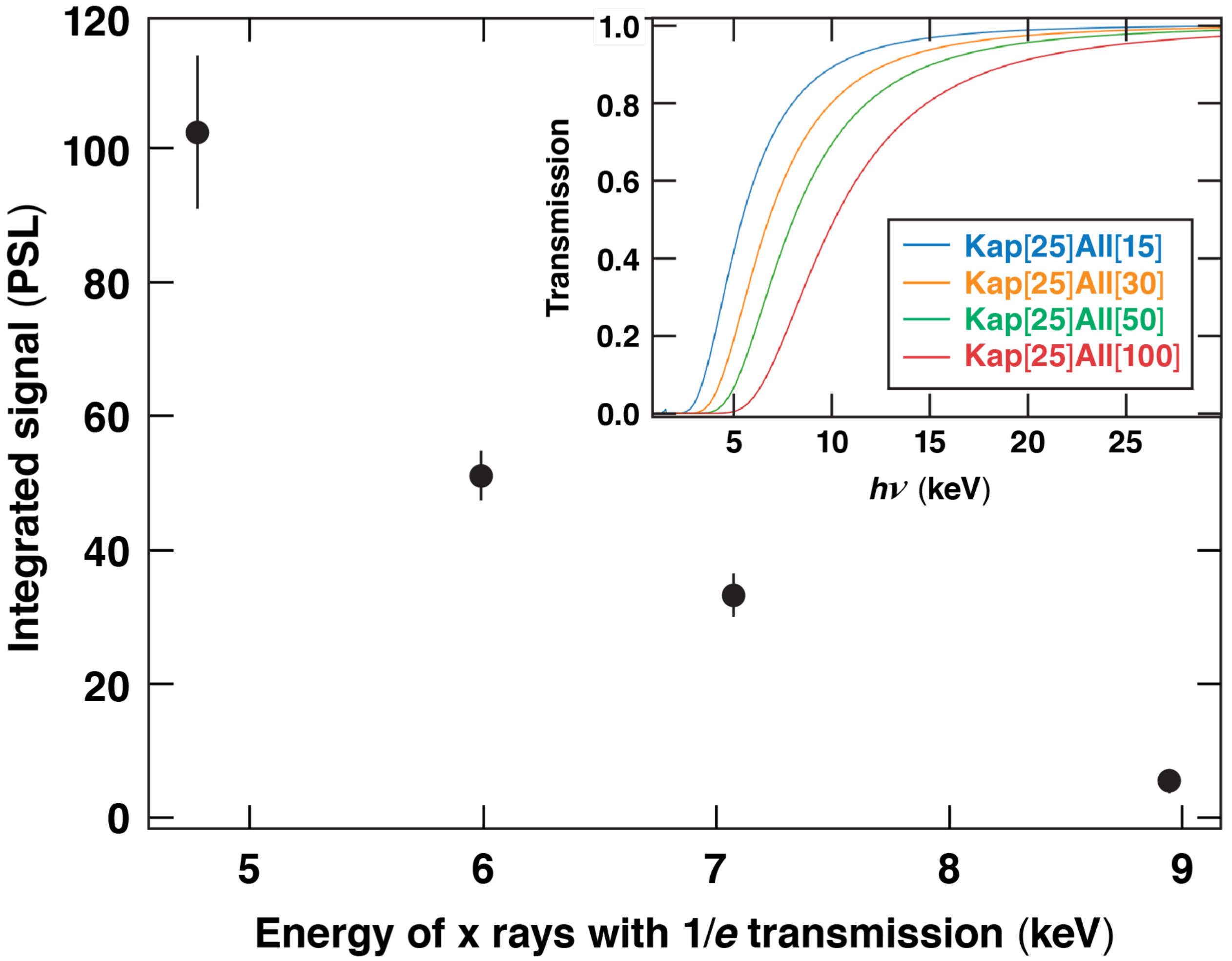

E28885

Temporal and spatial measurements of the x-ray emission were made using a fast x-ray framing camera*

40-ps gate width
46 pinhole array
10-μm pinholes
6× magnification

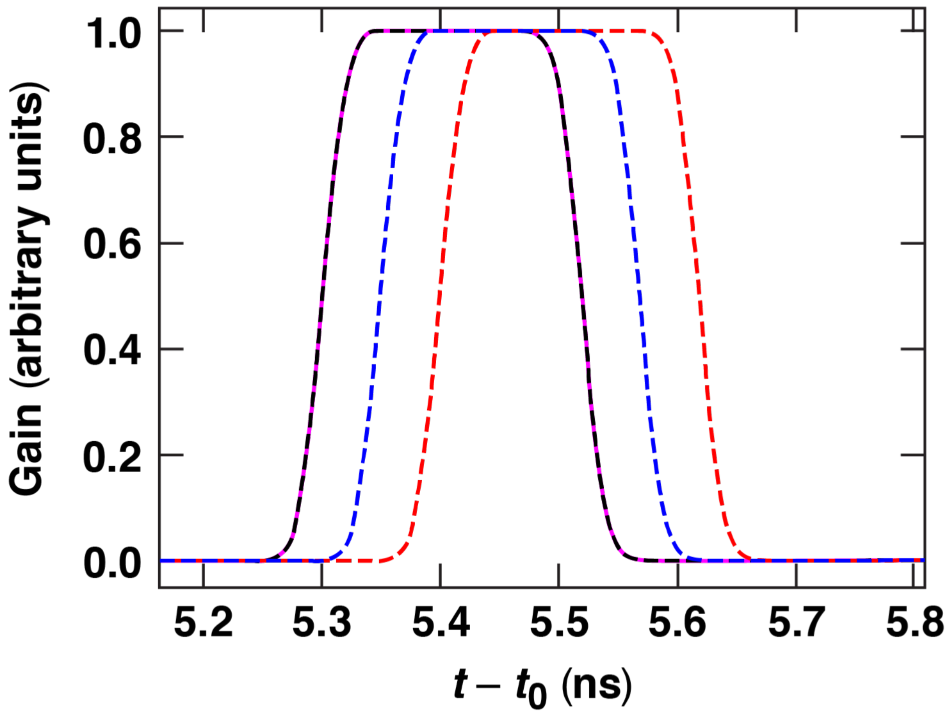

E28886

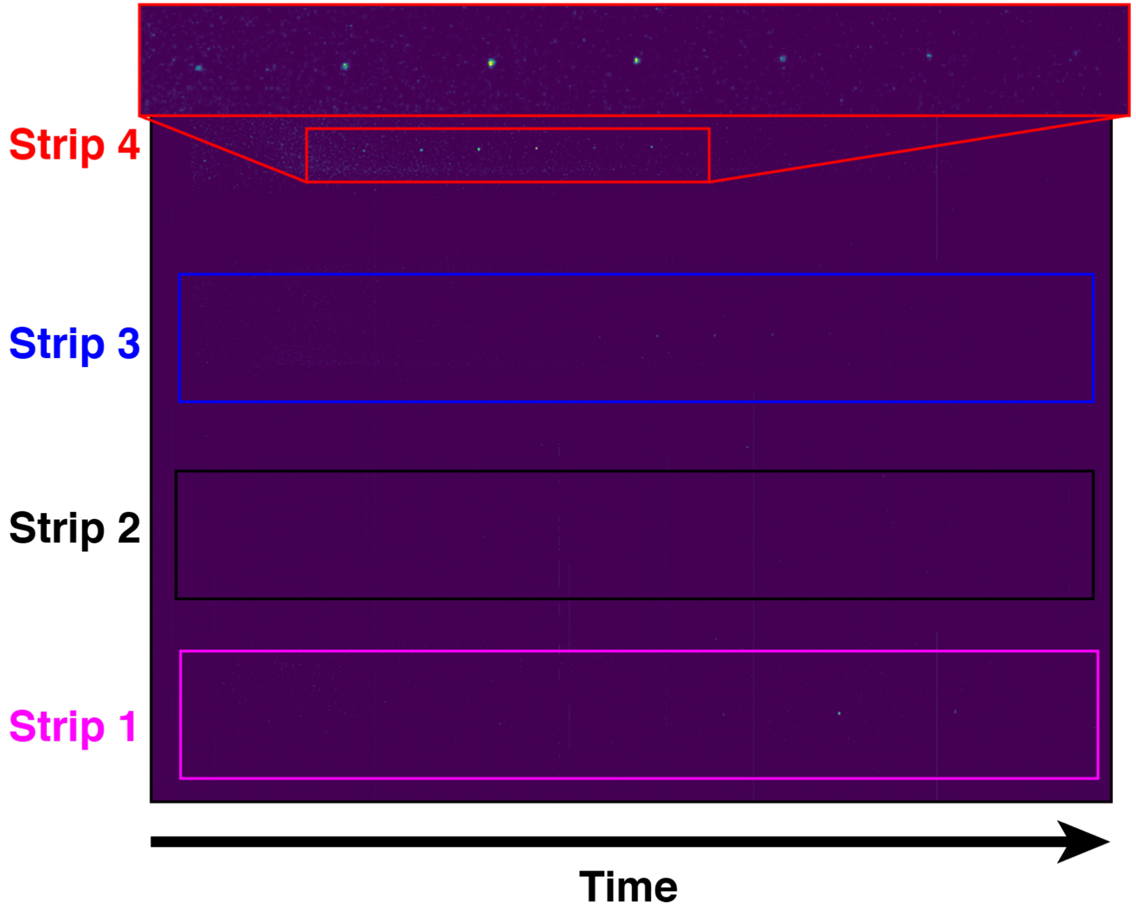

E28887

*Sydor Technologies, Fairport, NY 14450-9100.

A shock collapse time of 5.5 ns and time-resolved radial profiles were measured

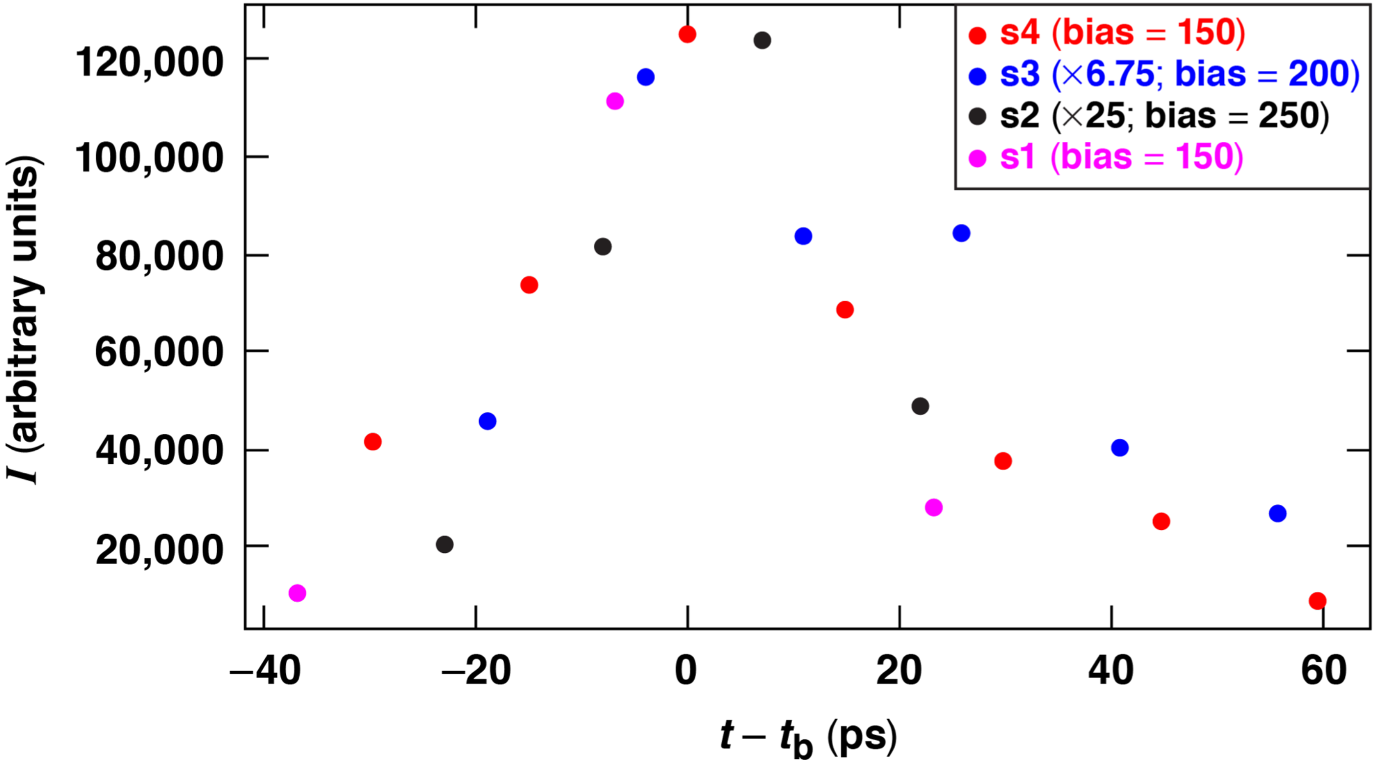

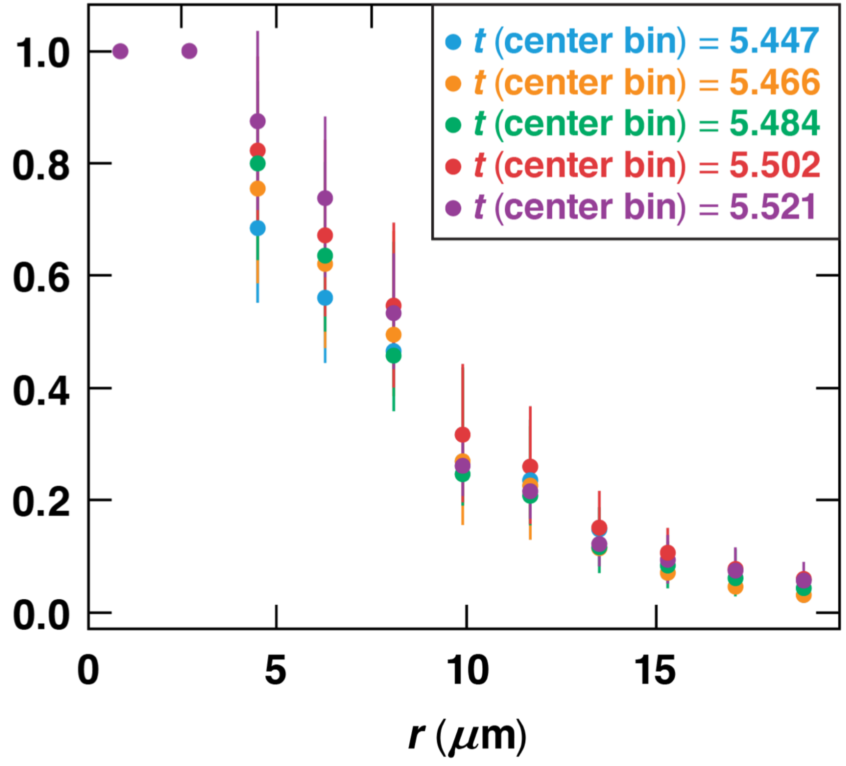

E28888

A forward-fitting procedure is used to generate data from the models to compare to the experimental measurements

- The models are used to generate temperature profiles (electron and ion) and density profiles
- These profiles are used to calculate neutron and x-ray emission profiles
- Instrument response functions are then applied to the emission profiles to generate predictions to compare to the measurements

$$\frac{d^2 N}{dt\, dV} = \frac{1}{2} n_{\mathrm{D}}^2 \langle \sigma v \rangle_{\mathrm{DDn}} \left[\frac{\text{neutrons}}{\text{m}^3\text{s}} \right]$$

$$J_v = \frac{\sqrt{2^{11}\pi^3}}{3} \frac{\left(\frac{e^2}{4\pi\varepsilon_0}\right)^3 \overline{Z}^2 n_{\mathrm{e}}^2}{m_{\mathrm{e}}^2 c^3 \overline{Z} \sqrt{3kT_{\mathrm{e}}/m_{\mathrm{e}}}} e^{-h\nu/kT_{\mathrm{e}}} \left[\mathrm{Js^{-1}\,m^{-3}\,Hz^{-1}}\right]$$

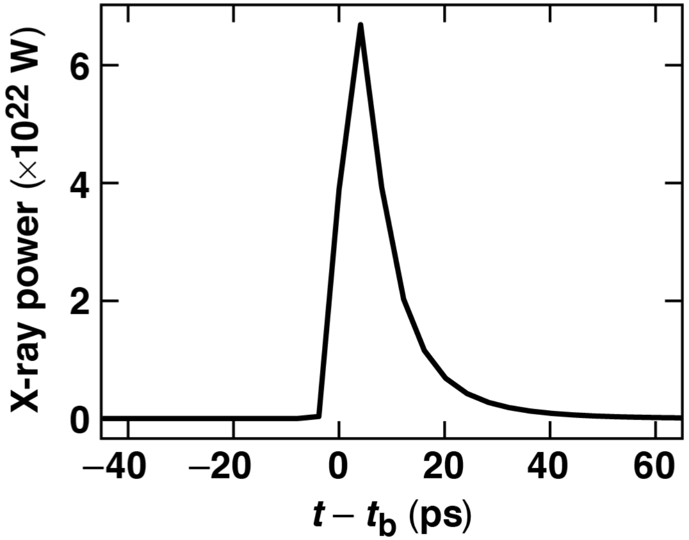

E28890

+ IRF

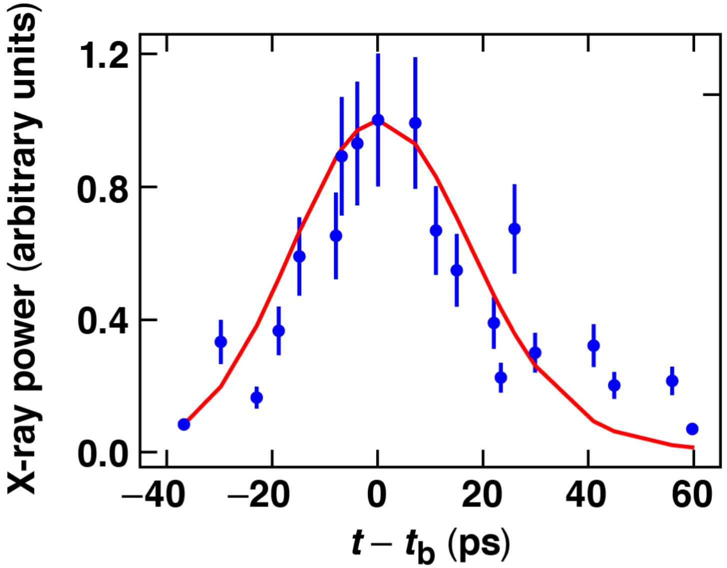

E28891

IRF: instrument response function

The measurements are fit using two models and a Bayesian model fitting method*

- Models include a semi-analytic modified Guderley solution** and a 1-D Lagrangian hydrodynamics code *LILAC*†
- The modified Guderley solution includes only hydrodynamics and electron–ion equilibration, while *LILAC* includes a full suite of physics including radiation transport and thermal conduction along with more-realistic equations of state
- A forward-fitting procedure is applied using a minimization of information with the inclusion of nuisance parameters

Physical parameters of interest

Data (experimental and modeled)

Experimental error

$$I(\theta \mid d_{\text{exp}})^{*} = \sum_i \frac{\left[d_{\text{exp},\,i} - d_{\text{m}}(\theta)_i\right]^2}{2\sigma^2_{\text{exp},\,i}}$$

Terms determining how nuisance parameters change information gained from the experiment

$$\left\{ \begin{aligned} & -\frac{1}{2}\left[d_{\text{exp}} - d_{\text{m}}(\theta)\right]^T \beta^T \beta \left[d_{\text{exp}} - d_{\text{m}}(\theta)\right] \\ & +\frac{1}{2}\ln\left(\left|\Lambda_\eta\right| \left|\alpha^T \alpha\right|\right) - \ln\left[P(\theta)\right] \end{aligned} \right.$$

Prior knowledge on physics parameters

*J. A. Gaffney *et al*., Phys. Plasmas 26, 082704 (2019).
** V. Gopalaswamy *et al*., Nature 565, 581 (2019).
† K. D. Humbird *et al*., Computer Science Archive, available at https://arxiv.org/abs/1812.06055 (2018).

X-ray shape is insensitive to the thermal conduction model used around shock collapse

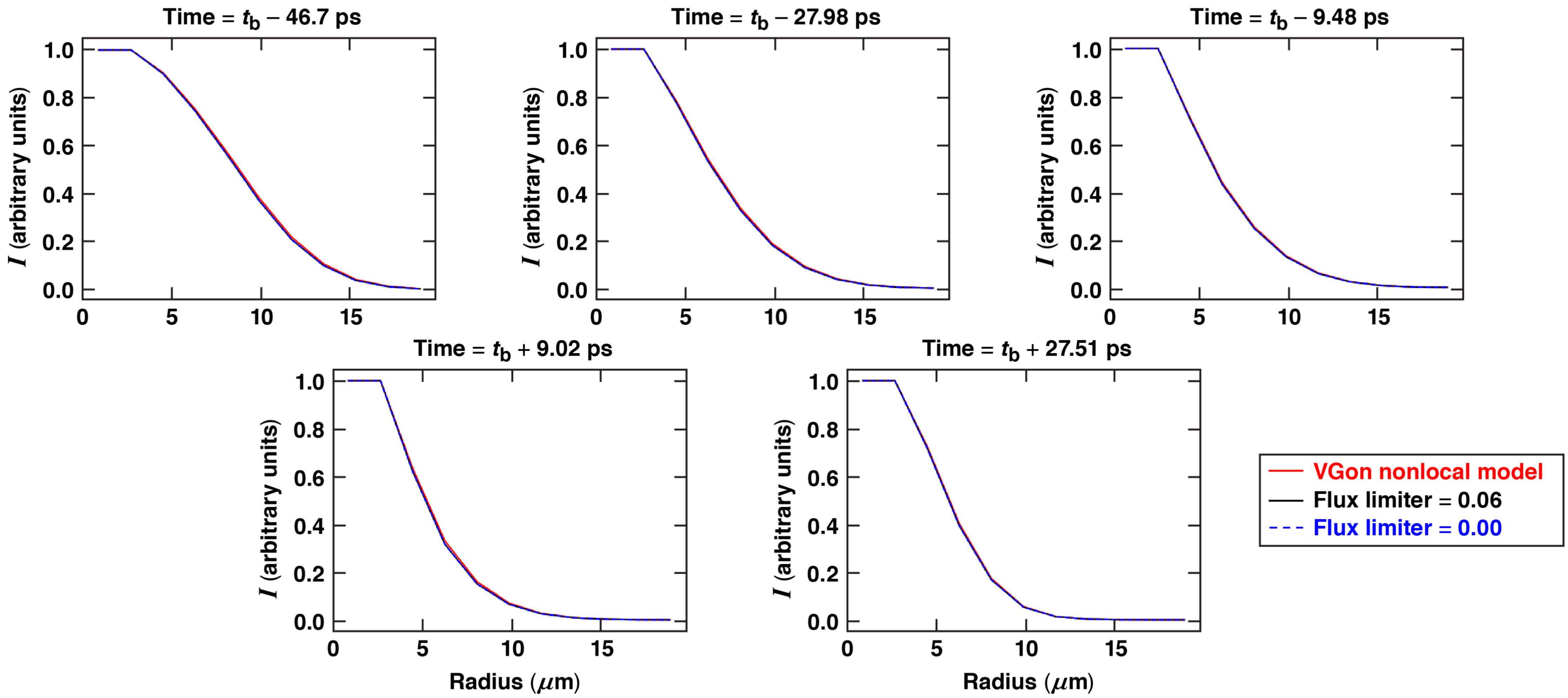

E28892

A very small amount of the internal energy is conducted around the time of shock collapse

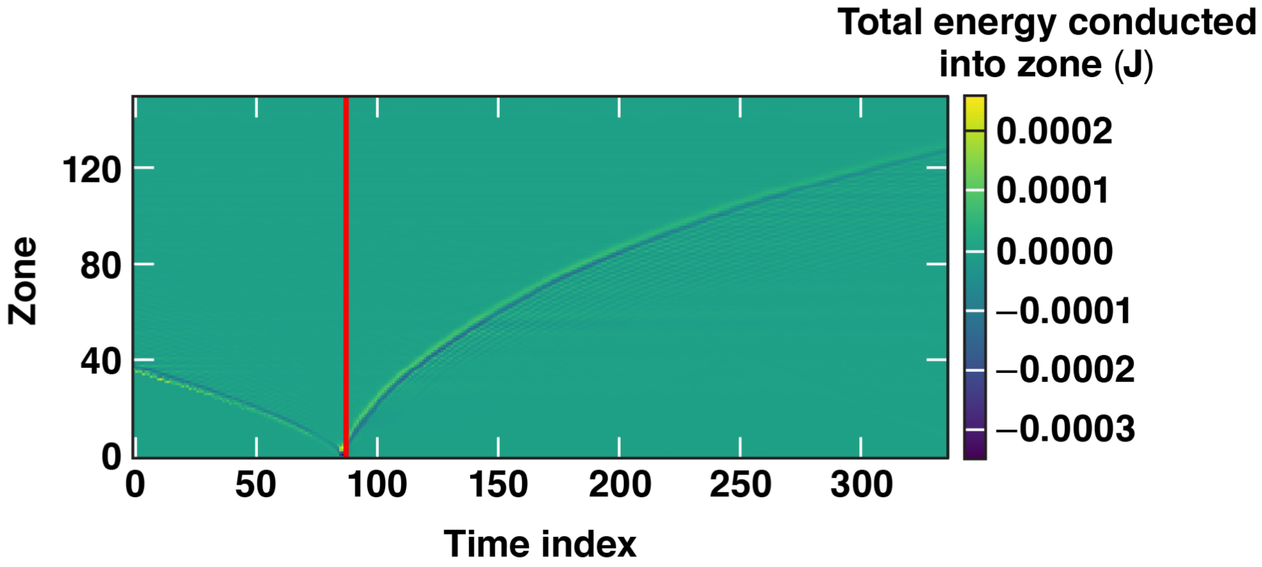

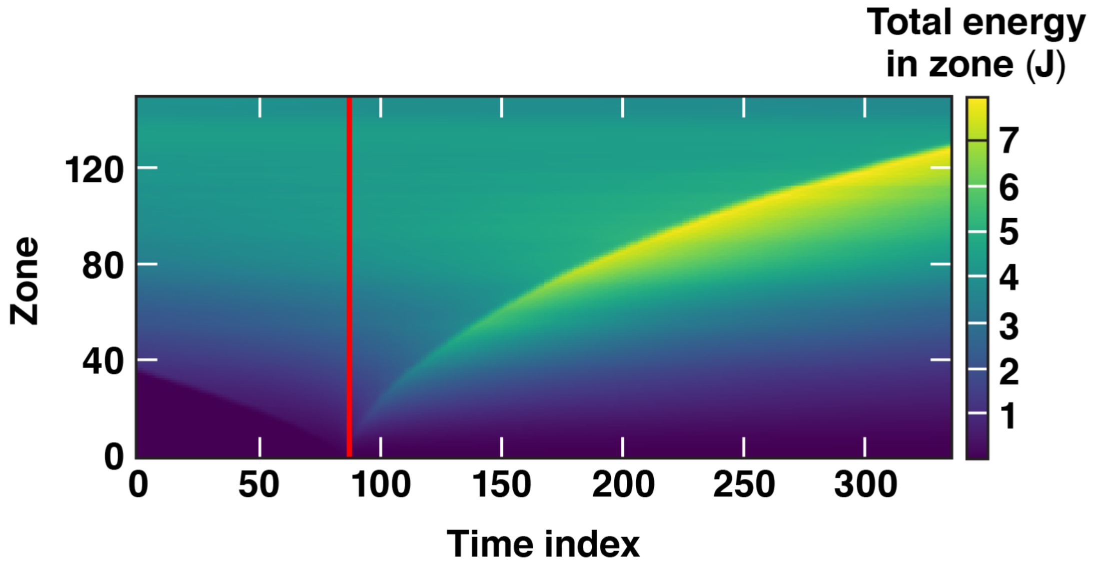

E28893

The conducted energy in the most-extreme cases accounts for a small fraction of a percent of total internal energy.

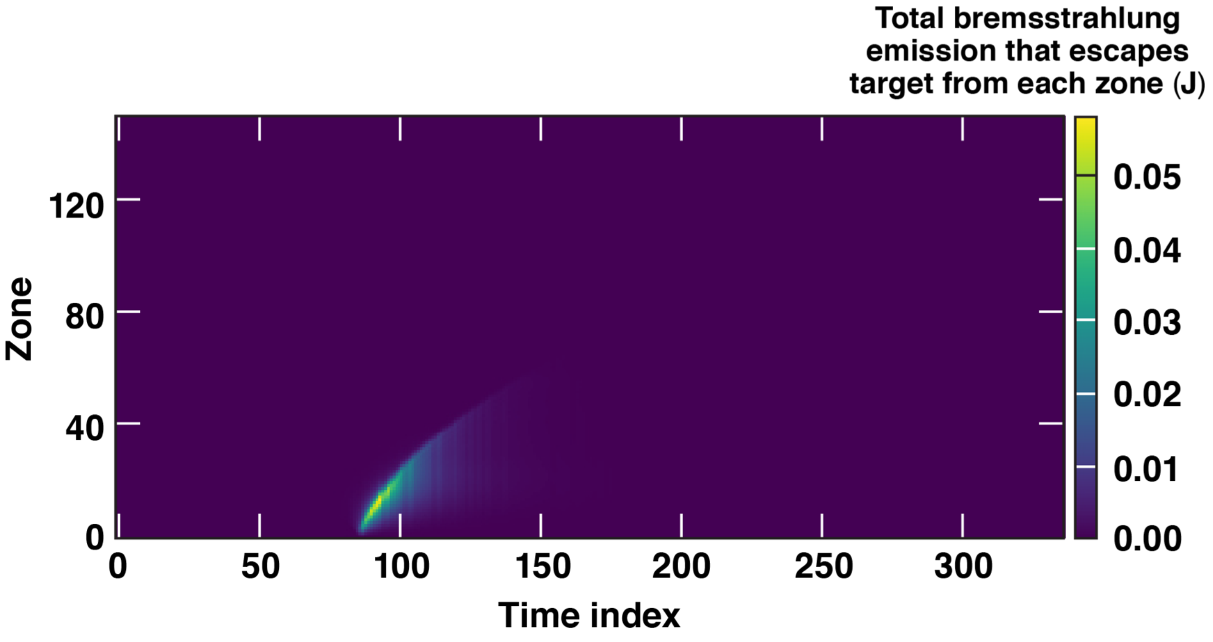

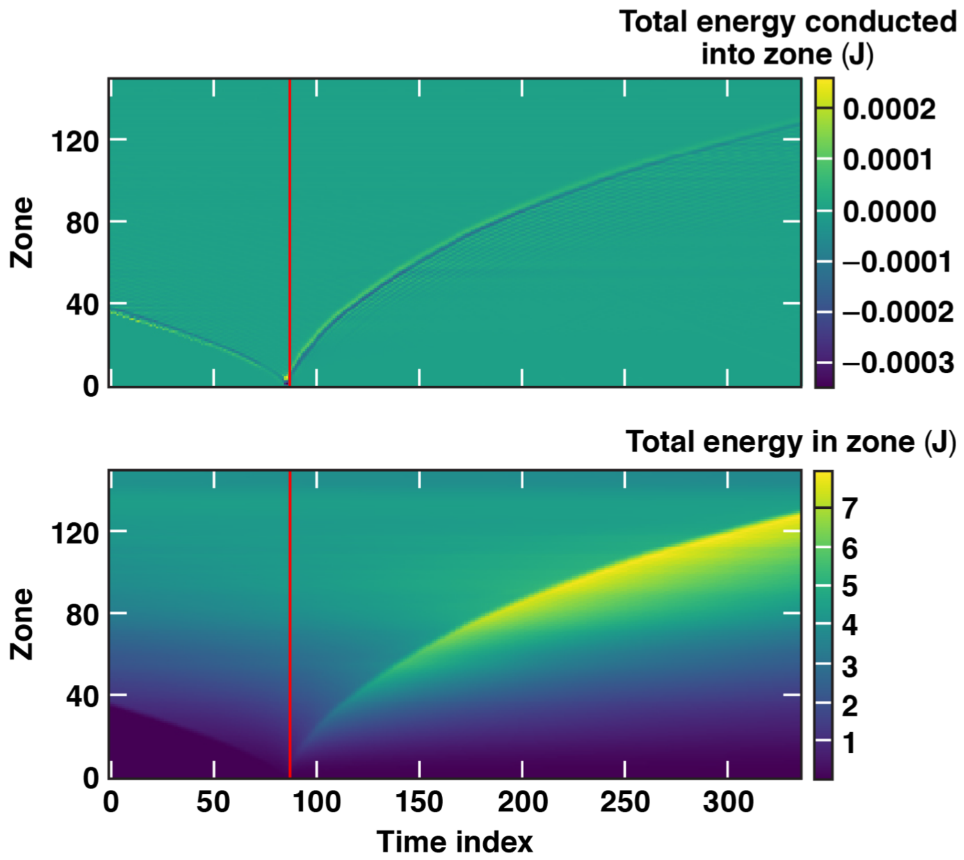

E28894

Emission follows the shock front closely, so the shape of the emission is likely dominated by the outgoing trajectory (which is determined by the EOS and the strength of the shock → Energy coupling in the corona?)